Journal of Visualized Experiments
Clarifying and Imaging Candida albicans Biofilms
--Manuscript Draft--

Article Type:	Invited Methods Article - JoVE Produced Video
Manuscript Number:	JoVE60718R1
Full Title:	Clarifying and Imaging Candida albicans Biofilms
Section/Category:	JoVE Immunology and Infection
Keywords:	Candida albicans; biofilm; refractive index matching; methyl salicylate; clarification; confocal microscopy
Corresponding Author:	Frederick Lanni, Ph.D. Carnegie Mellon University Pittsburgh, PA UNITED STATES
Corresponding Author's Institution:	Carnegie Mellon University
Corresponding Author E-Mail:	lanni@cmu.edu
Order of Authors:	Frederick Lanni, Ph.D.
	Katherine Lagree
	Manning Y. Huang
	Lan Yan
	Carol A. Woolford
	Aaron P. Mitchell
Additional Information:	
Question	Response
Please indicate whether this article will be Standard Access or Open Access.	Open Access (US$4,200)
Please indicate the **city, state/province, and country** where this article will be **filmed**. Please do not use abbreviations.	Pittsburgh, Pennsylvania, USA

TITLE:

Clarifying and Imaging *Candida albicans* Biofilms

AUTHORS AND AFFILIATIONS:

Frederick Lanni[1], Katherine Lagree[1], Manning Y. Huang[1], Lan Yan[2], Carol A. Woolford[1], Aaron P. Mitchell[1]

[1]Department of Biological Sciences, Carnegie Mellon University, Pittsburgh, PA, USA

[2]Center for New Drug Research, Department of Pharmacology, School of Pharmacy, Second Military Medical University, Shanghai, P. R. China

Corresponding Author:

Frederick Lanni   (lanni@cmu.edu)

Email Addresses of Co-Authors:

Katherine Lagree   (klagree@andrew.cmu.edu)

Manning Y. Huang   (manningh@andrew.cmu.edu)

Lan Yan   (ylansmmu@sina.com)

Carol A. Woolford   (cw2g@andrew.cmu.edu)

Aaron P. Mitchell   (apm1@cmu.edu)

KEYWORDS:

Candida albicans, biofilm, refractive index matching, methyl salicylate, clarification, confocal microscopy

SUMMARY:

To view and quantify the internal features of *Candida albicans* biofilms, we prepare fixed intact specimens that are clarified by refractive index matching. Then, optical sectioning microscopy can be used to obtain three-dimensional image data though the full thickness of the biofilm.

ABSTRACT:

The microbial fungus *Candida albicans* can undergo a change from commensal colonization to virulence that is strongly correlated with its ability to switch from yeast-form growth to hyphal growth. Cells initiating this process become adherent to surfaces as well as to each other, with the resulting development of a biofilm colony. This commonly occurs not only on mucosal tissue surfaces in yeast infections, but also on medical implants such as catheters. It is well known that biofilm cells are resistant to antifungal drugs, and that cells that shed from the biofilm can lead to dangerous systemic infections. Biofilms range from greatly translucent to opaque due to refractive heterogeneity. Therefore, fungal biofilms are difficult to study by optical microscopy. To visualize internal structural, cellular, and subcellular features, we clarify fixed intact biofilms by stepwise solvent exchange to a point of optimal refractive index matching. Use of methyl salicylate allows sufficient clarification (n = 1.537) to enable confocal microscopy from apex to base in 600 μm with little attenuation for *C. albicans* biofilms. In this visualization protocol we outline phase contrast refractometry, the growth of laboratory biofilms, fixation, staining,

45 solvent exchange, the setup for confocal fluorescence microscopy, and representative results.
46
47 **INTRODUCTION:**
48 *Candida albicans* is a microbial fungus that is typically commensal in humans. It is of fundamental
49 interest to biologists because the organism has multiple morphologies. For example, in response
50 to certain environmental cues or stressors, yeast-form budding cells will switch to filamentous
51 growth as septating chains of highly elongated cells known as hyphae. The transition is important
52 as an example of phenotypic expression of a changeover between a unicellular and multicellular
53 gene expression program. Likewise, *C. albicans* is of biomedical interest because the organism is
54 a well-known opportunistic pathogen. It is responsible for mucosal yeast infections such as thrush
55 (oral candidiasis), genitourinary infections, and a cause of dangerous invasive or systemic
56 infections in immunologically weakened patients.
57
58 This organism's potential for virulence is closely connected to its multiple morphotypes and other
59 aspects of its genetic versatility[1-4]. Germ tube extension, the first visible stage of the transition to
60 hyphal growth, occurs with sufficient rapidity to enable engulfed *C. albicans* cells to break out of
61 phagocytes and thereby escape an early phase of the cellular immune response of the host[5].
62 Additionally, filamentation is preceded and accompanied by a large increase in cell-to-cell and
63 cell-to-surface adherence that is due to regulated expression of several classes of cell wall
64 proteins known as adhesins[6–9]. Under a wide variety of conditions, the combination of adherence
65 and filamentation results in a dramatic shift from planktonic, unicellular growth to surface-
66 associated colonial growth that forms a biofilm. *C. albicans* biofilms may develop on common
67 implanted medical devices such as venous catheters. Disseminated infections can result when
68 such biofilms begin to bud off yeast-form cells and shed them into circulating blood. Multiple
69 studies have shown that biofilm cells are more resistant to antifungal drugs than planktonic
70 cells[10,11], which may be due in part to lowered metabolism[12]. Furthermore, the high overall
71 adherence of a biofilm may provide the anchoring needed for efficient invasive growth of hyphae
72 into host tissue[1].
73
74 Optical clarification of *C. albicans* biofilms by refractive index matching has had a major impact
75 on our ability to visualize the structure of this microbial community and discover relationships
76 between gene expression and phenotype. Biofilms grown in the laboratory on test surfaces under
77 liquid culture medium for 48 h appear as a whitish coating that is dense enough and thick enough
78 to be opaque (**Figure 1**). Therefore, many interesting phenotypic features of the biofilm are
79 hidden from view. The 24 h wild type biofilms grown in YPD, RPMI-1640, or Spider medium at 37
80 °C range up to 300 μm thick, with 48 h biofilms often reaching 500 μm. The opacity is due to light
81 scattering, which arises from refractive heterogeneity: the fungal cell wall is more refractive than
82 the surrounding medium, and the cytoplasm slightly more refractive than the cell wall. The
83 resulting high optical density of a native biofilm obscures all structures more than 30 μm deep
84 when viewed with a conventional microscope or even a confocal scanner (**Figure 2**). However, a
85 large degree of clarification can be achieved by infiltrating fixed biofilms with a high refractive
86 index liquid that approximately matches the refractivity of major cellular constituents. After
87 clarification, imaging at submicron resolution can be carried out by confocal microscopy through
88 the entire thickness of almost any *C. albicans* biofilm[13]. In wild type specimens, it is easy to see

89 that biofilms consist of long entangled hyphae, clusters of budded yeast-form cells or
90 pseudohyphal cells, void spaces, and some amount of extracellular matrix. Moreover, biofilms
91 generally are stratified, showing spatially variant morphological differences in cell type, cell
92 density, and the presence of budding or branching cells. Many variations in one or more of these
93 features have been observed in biofilms developed by mutant strains[14,15]. Additionally, reporter
94 strains show in situ spatial differences in gene expression[16,9,13]. The surprising degree of
95 clarification obtainable with this relatively simple and inexpensive approach also makes it
96 possible to see that many biofilms include apical hyphae and basal invasive hyphae extending out
97 to millimeter distances.
98
99 In this visualization protocol, we demonstrate the fixing, labeling, clarification, and imaging of a
100 *C. albicans* biofilm using a simple cell wall marker as a stain. The origin of the present version of
101 the protocol is the improved clarity we observed when formaldehyde-fixed biofilms were
102 infiltrated with 97% glycol methacrylate (GMA), which was then polymerized to embed the
103 biofilm in a hard plastic having a moderately high refractive index (n = 1.49). We then used
104 conventional phase contrast microscopy and a series of refractive index reference liquids to more
105 accurately determine the point of contrast reversal (maximum transparency) of the biofilm
106 (**Figure 3**). For *C. albicans* biofilms this occurred close to n = 1.530, which was surprisingly high
107 given that a dense protein structure such as hair keratin is only slightly more refractive (1.54–
108 1.55). Though it is on the upper end of the optimal range in **Figure 3**, we adopted methyl salicylate
109 (oil of wintergreen, n = 1.537) in the current protocol because it has long been used as a clarifying
110 agent for microscopy in embryology and histology, it has low toxicity and low vapor pressure,
111 and it gave excellent results in our trials using moderate-NA oil immersion optics.
112
113 Four points should be made here:
114
115 (1) With few exceptions, the ideal situation in microscopy is that the refractive index of the
116 specimen should be equal to the refractive index of the objective lens immersion fluid[17,18,13]. For
117 three-dimensional (3D) imaging studies where deep focusing is necessary, this is always
118 important.
119
120 (2) Our experimental result for optimal clearing (n = 1.525–1.535) is slightly higher than standard
121 immersion oils (n = 1.515, 1.518) and therefore violates point (1), and thus introduces a source
122 of spherical aberration when using standard oil immersion optics. One solution to this problem
123 is use of an objective designed for an immersion index in the higher range. Because of a
124 resurgence of interest in imaging cleared specimens, specialty objectives with the needed
125 correction are becoming available. The other solution is to adjust the index of the clarifying
126 medium down to 1.515 or 1.518 by the addition of a small amount of butanol (n = 1.399) for
127 optimal oil immersion performance, and accept the slightly degraded clarity.
128
129 (3) Microscopy of intact biofilms (and other specimens on this scale) requires a significant
130 working distance to accommodate the specimen thickness. This is a major practical
131 consideration. A long working distance limits the optics to a moderate numerical aperture (NA =
132 0.6–1.25), which limits resolution but also limits the severity of spherical aberration.

(4) The optimal refractive index for clarification may be different for other types of fixed specimens. Specimens should be tested accordingly using phase contrast and a series of refractive index reference liquids as shown in **Figure 3**.

PROTOCOLS:

1. Growth of biofilm cultures

CAUTION: *Candida albicans* is a human pathogen. At some institutions, culture of this organism requires BSL-2 containment.

1.1. Streak out selected strain on a yeast extract-peptone-dextrose (YPD) agar plate and grow 48 h at 30 °C.

1.2. Select single colonies from the plate to inoculate 5 mL of YPD medium in 15 mL culture tubes for overnight aerobic growth (carousel rotator, 52–55 rpm) at 30 °C.

1.3. Determine cell density using a 40- to 50-fold dilution of the overnight culture. Compute the dilution factor needed to bring the cell density to 3×10^6 cell/mL for silicone substrata, or 0.6–1.2×10^6 cells/mL for cover glass surfaces treated with concanavalin-A (ConA) or wheat-germ agglutinin (WGA) (see Discussion).

1.4. For biofilm growth in a 12 well plate (**Figure 1**), dispense 2.0 mL of sterile filamentation medium into each well, and warm the plate to 37 °C in a humidified incubator. A variety of media will induce filamentation, more strongly at an elevated temperature (37 °C) and with added serum. Fetal bovine serum (FBS) is recommended. Recommended media are YPD, Spider-Mannitol, or RPMI-1640.

1.5. With sterile tweezers, place a prepared substratum into each well in the warmed plate and dislodge bubbles. Add the inoculum from the overnight culture to reach the cell density recommended in step 1.3 in each well. One well without inoculum serves as a visual blank and control against contamination.

1.6. Place the plate on a 60 rpm orbital mixer in a humidified 37 °C air incubator for 90 min to allow time for cell adhesion. After 90 min, remove the medium and unattached cells, wash with sterile medium or phosphate-buffered saline (PBS), and place inoculated substrata into culture dishes or another multiwell plate containing prewarmed filamentation medium. With multiwell plates, it is very convenient to use a second plate for the wash step and a third plate with 2.0 mL of prewarmed medium per well to receive the washed inoculated substrata. Sterilize tweezers prior to each transfer.

1.7. Return the plate to the 37 °C humidified ambient-air incubator and grow the biofilms up to 48 h with 60 rpm orbital mixing for aeration. There should be little planktonic growth in each

177 culture unless the developing biofilm is shedding yeast-form cells. A biofilm grown in this way is
178 shown in **Figure 1**.

179

180 **2. Specimen processing for imaging**

181

182 CAUTION: Aldehyde fixatives are volatile and hazardous. Prepare fixative dilutions in a fume
183 hood, not in a biosafety cabinet. Do not put fixatives into incubators used for live cells. Work with
184 diluted fixatives in covered dishes in a fume hood or a well-ventilated benchtop area. Dispose of
185 fixatives and post-fix wash solutions as hazardous waste.

186

187 2.1. Prepare fresh fixative, 4% formaldehyde or paraformaldehyde in PBS, optionally with up to
188 2% glutaraldehyde. Formalin diluted to 4% may be used for routine work.

189

190 NOTE: Glutaraldehyde in particular will increase broadband autofluorescence and may attenuate
191 the fluorescence of expressible tags such as dTomato.

192

193 2.2. Remove the culture medium from the specimen and replace with PBS to dilute away serum
194 proteins, or transfer the biofilm on its substratum to PBS, for several minutes.

195

196 2.3. Transfer the specimen into fixative, and set the covered dish on a slow orbital mixer for 20
197 min. Extend the time period when processing thicker specimens (see Discussion). Sufficient
198 fixative volume should be added to each dish to immerse all biofilm growth, including any on the
199 inner sides of the dish.

200

201 2.4. Remove the fixative and refill the dish with PBS to wash out the residual fixative. Dispose of
202 the fixative as hazardous waste. Repeat several short-term washes, then longer washes to allow
203 time for the residual fixative to diffuse out of the biofilm or agar block. The wash period depends
204 on the time allowed for fixation (see Discussion).

205

206 2.5. The needed quantity of stain will depend on the biofilm mass. Remove all biofilm from non-
207 specimen areas of the culture dish prior to staining, or transfer the fixed specimen into a new
208 dish ahead of staining. Do not allow the biofilm to drain or dry by keeping it immersed in PBS.

209

210 2.6. Add the stain to the dish (see Discussion) and set the covered dish on a slow orbital mixer
211 overnight (see Discussion). Protect from light.

212

213 2.7. In the morning, remove the staining solution and refill the dish with PBS to dilute the
214 unbound stain. Set the dishes on slow orbital mixer to destain for several hours.

215

216 **3. Clarification protocol: biofilms on impermeant substrata**

217

218 3.1. Clarified biofilms are hard to discern visually. Therefore, if desired, mark one side of each
219 substratum with a scratch to designate the side for inoculation.

220

3.2. Use labeled long Pasteur pipettes for all subsequent waste and solvent transfers to avoid cross contamination of the solvents.

3.3. Using tweezers, transfer the fixed biofilm from PBS to 5 mL of 50:50 PBS:methanol in a 20 mL glass vial with the biofilm facing up. Manually mix with orbital motion at 1 min intervals for 5 min (see Discussion).

3.4. Remove the solvent to a waste bottle, being cautious to avoid contact between the pipette and biofilm, or the biofilm and vial. Gently refill with 3 mL of neat methanol. Manually mix with orbital motion at 1 min intervals for 3 min.

3.5. Remove the solvent to a waste bottle, and immediately refill with 5 mL of methanol. Manually mix with orbital motion at 1 min intervals for 5–10 min. Remove the solvent to the waste bottle, and immediately refill with 3 mL of methanol. Biofilms often look more opaque at this point than their initial appearance.

3.6. Remove the solvent to the waste bottle, and immediately refill the vial with 5 mL of 50:50 methanol:methyl salicylate. Manually mix with orbital motion at 1 min intervals for 5–10 min. The biofilm should be semitransparent in this mixed solvent.

3.7. Remove the solvent to a waste bottle. Gently refill the vial with 3 mL of neat methyl salicylate (MS). Manually mix with orbital motion at 1 min intervals for 3 min.

3.8. Remove the solvent to the waste bottle, and immediately refill with 5 mL of neat MS. Manually mix with orbital motion at 1 min intervals for 5–10 min. At this point, the biofilm should be transparent. Remove the solvent to the waste bottle, and immediately refill the vial with 3 mL of neat MS. The processed biofilm is stable in this solvent.

3.9. For biofilms on agar (see Discussion) extend all exchange time periods to allow for water and solvent diffusion though the agar. The necessary time periods can be estimated using a low-power dissecting microscope with darkfield illumination to view the solvent advance into the agar. The protocol achieves good clarification and no major shrinkage effects when 2% agar is used, but the clarified agar will condense if squeezed while handling with tweezers. Use of a spatula is recommended.

4. Imaging setup for confocal microscopy

4.1. The following steps are for the use of an inverted microscope. Use a solvent-proof dish that has a cover glass bottom to hold the inverted specimen on the microscope stage (see Discussion).

4.2. Prepare spacers for support of the inverted specimen. Use small rectangles cut from microscope slides (1,000 µm thick), cover glasses (170 µm), or 13 mm silicone rings (330 µm, see **Table of Materials**), which may be stacked as needed. Presoak the rings in methyl salicylate for 1 h to minimize focus drift due to swelling.

265

266 4.3. For a biofilm on a medical grade silicone square, invert the square (i.e., turn it biofilm down)
267 and set it on a spacer in a pool of methyl salicylate in the dish (**Figure 2**). Make sure to avoid any
268 bubbles below the specimen.

269

270 4.4. Mount the dish firmly on the stage of the microscope and make oil immersed contact with
271 the objective (see Discussion).

272

273 4.5. Adjust the amount of MS in the dish so that the meniscus holds the specimen firmly down
274 on the spacer by surface tension. Place a droplet of MS on top of the inverted square substratum
275 to reduce light scatter from the matte finish, and cover the dish with a glass plate to limit
276 evaporation. Wait several minutes for the specimen to settle onto the spacers prior to imaging.

277

278 4.6. Use transmitted light to visually inspect the field of view and locate the current focus position
279 relative to the apical and basal regions of the inverted biofilm. Set the condenser illuminating
280 numerical aperture (INA) to a minimum (close down the condenser iris) to increase contrast,
281 otherwise the clarified biofilm will be nearly invisible. When done, switch off the transmitted light
282 source.

283

284 4.7. Switch over to confocal fluorescence and set the lower and upper limits of the serial-focus
285 image stack needed to span the biofilm. Upward focus drive stepping, which is recommended,
286 will first show dislodged cells that have settled onto the cover glass and very long apical hyphae
287 that are resting on the glass. At the upper end of the sequence, the founder cells should be seen
288 adhered to the substratum at the base of the biofilm. Set the pinhole diameter, the pixel spacing
289 in the image plane, and the focus step increment using the general criteria outlined in the
290 Discussion.

291

292 **REPRESENTATIVE RESULTS:**
293 Biofilms such as that in **Figure 1** are heavily translucent to opaque, but are routinely clarified and
294 imaged by employing the protocol above. **Figure 2** shows the strong attenuation of fluorescence
295 with focus depth in a fixed biofilm in PBS, compared to the same biofilm after index matching. As
296 shown in **Figure 3**, using serially miscible solvents of increasing refractive index the maximum in
297 clarity can be quickly estimated. This is refined by conventional phase contrast microscopy to find
298 the point of minimum contrast (maximum transparency). It is evident that this optimum is not
299 achieved by homogeneous index matching. This is because subcellular structures differ slightly in
300 refractive index. In this case, contrast reversal occurred in the cell wall at a slightly lower solvent
301 index than in the cytoplasm. For *Candida albicans* biofilms, the optimum occurs close to n =
302 1.530. The 48 h wild type and *cak1* DX mutant biofilms in **Figure 4A** were 500 μm in thickness,
303 yet the yeast cells at the base were imaged nearly as sharply as the apical cells. Likewise, as shown
304 in **Figure 4C**, attenuation of fluorescence was not strongly correlated with focus depth. **Figure 5**
305 shows invasive hyphae in agar, hundreds of micrometers below a surface biofilm. Mature
306 invasive hyphae consistently produce lateral budding yeast proximal to the septa in the hyphal
307 chain, giving rise to subcolonies of yeast-like cells at regular intervals along an invasive hypha.

308

FIGURE LEGENDS:

Figure 1: Biofilm cultures prior to clarification. A 24 h biofilm grown from an isolate of a complemented *efg1 Δ/Δ* strain of *C. albicans* in a 12 well plate on a silicone square in RPMI-1640 liquid medium supplemented with 10% FBS. The sterile blank is in well C4 (inset). Cut cross section of 96 h wild type biofilm grown in a 6 well plate on a 3.75 mm agar base in the same medium showing invasive hyphae. Both panels are to the same scale. Scale bar = 2.0 mm.

Figure 2: Improvement of deep imaging by index matching. The figure shows sideview projections of confocal image stacks from a 48 h wild type biofilm that was fixed and stained with ConA-Alexafluor 594. (**A**) The specimen was imaged in PBS using a 63x 1.0 NA direct water-immersion objective. Attenuation was severe at a focus depth of 30 μm. (**B**) After clarification by protocol steps 3.3–3.6, the same biofilm was imaged in methyl salicylate with minimal attenuation using a 40x 0.85 NA oil immersion objective. After background subtraction and sideview projection of the 3D image stacks, the 40x data was spatially rescaled to match the 63x data for comparison. (**C**) Schematic diagram showing inverted mounting of the cleared specimen (from MS) by transfer to MS in a black-anodized aluminum dish with a cemented cover glass bottom (see Discussion). Scale bar = 50 μm.

Figure 3: Phase contrast refractometry shows contrast reversal of cellular features in the range of optimum index matching. Fixed biofilms on cover glasses were exchanged from PBS into methanol, then into xylene (n = 1.496). These biofilms were then exchanged one each from xylene into a set of refractive index reference liquids (Series E, Cargille Laboratories, see **Table of Materials**) and visually examined side-by-side to determine the index range giving highest transparency. (upper panel) Phase contrast images: One biofilm was serially exchanged between xylene and a narrow set of reference liquids in that range. After each exchange, the same field was relocated and viewed though a cover glass using a 40x 0.85 NA Ph2 oil immersion phase contrast objective and Ph2 condenser. All images were recorded with the same lamp setting and camera exposure to accurately display changes. With increasing index, contrast reversal is first seen at n = 1.530 for the cell wall, followed by cytoplasm at n = 1.535. Scale bar = 10 μm. (lower panel) Graph showing the minimum in average biofilm brightness at the point of maximum transparency. Strong scattering of light within the biofilm causes the average brightness to exceed the blank field. Isolated cells appear darker than the blank field, up to contrast reversal in the range 1.530–1.535.

Figure 4: Deep imaging of mutant and wild type *C. albicans* biofilms. A wild type strain (DAY185) and a cell cycle related protein kinase diminished expression strain (*cak1* DX)[14] were grown at 37 °C for 48 h on silicone substrata in liquid YPD medium. The biofilms were fixed, stained with ConA-Alexafluor 594, and clarified using the solvent exchange protocol into methyl salicylate. The 3D confocal microscopy showed that both biofilms were ~500 μm thick. Image data were converted to 32-bit format in ImageJ or Fiji (https://imagej.nih.gov/ij/ or http://fiji.sc), then processed using the **Subtract Background** function with a 50-pixel rolling ball radius, thresholding to set negative pixels to zero, reslicing, and using maximum intensity projection to produce side views. (**A**) Axial and side-view projections: The wild type biofilm grew to a thickness of 502 μm as seen in the side view projection of the 558-plane confocal image stack. Scale bar = 100 μm. (left hand panels) 40-

plane axial projections from apex (top) to base (bottom) show the variation in cell types in different strata of the biofilm. This example showed characteristic wild type structure: adherent cells at the base give rise to hyphae that ascend into a dense middle zone of pseudohyphal and yeast-like cells. Above the midzone, hyphae reemerged and gave rise to clusters of budding yeast. The long hyphae seen in the apical zone likely extended into the culture medium in the living biofilm, but folded over onto the surface of the biofilm during specimen processing. The *cak1* DX biofilm grew to a thickness of 500 μm as seen in the side-view projection of the 556-plane image stack. This mutant, which is known to undergo filamentous growth in the absence of inducing stresses[14], produced a dramatically different architecture. As seen in both the sideview and axial projections (right hand panels), many branching cells gave rise to radial outgrowths. (**B**) Examples of branching hyphae within the *cak1* DX biofilm. Scale bar = 10 μm. (**C**) Fluorescence attenuation with depth in the clarified wild type biofilm was quantified by masking out background pixels, then computing the average digital signal for all non-background pixels in each image plane. With the exception of apical hyphae that are brightly tagged by the lectin, there was no strong attenuation trend with focus depth.

Figure 5: Invasive hyphae in agar. *C. albicans* hyphae in a surface biofilm will penetrate an agar substratum to millimeter distances (see **Figure 1**). After clarification, invasive structures may be viewed downward though the biofilm, or upward from the bottom side of the agar. The latter demands greater working distance. Alternatively, after fixation but prior to staining and solvent exchange, the agar may be cut vertically with a scalpel or razor blade into 1–2 mm slabs that then can be turned on a side and imaged directly in side view after staining and clarification. This procedure is recommended. In this projection of a 213 μm square field of view, a rainbow color scale was used to encode axial position over a 75 μm range: blue features are near and red features are deeper into the plane of the page. This view shows that long hyphae bud off lateral yeast-form cells at semiregular intervals that give rise to subcolonies. Scale bar = 50 μm.

Table 1: Confocal pinhole diameter, transverse sampling, and axial sampling values for a 600 nm emission wavelength.

DISCUSSION:
Advances in fluorescence microscopy in optical sectioning, resolution, speed, avoidance or compensation of aberration, multichannel acquisition, and in computing power, have caused a resurgence in imaging intact specimens. For fixed specimens, both classical and novel clarification and expansion methods have had a major impact[19-24]. In this case, we applied a fast and simple solvent-based index matching approach to study the structure of fungal biofilms that are heavily translucent to opaque.

The preceding protocols have been tested with a range of specimens. In our laboratory *Candida albicans* biofilms are most often grown on 14 mm squares cut from a sheet of medical grade silicone rubber (see **Table of Materials**). This substratum is used because growth on PDMS (poly-dimethylsiloxane) submerged in liquid culture medium has been established as an important in vitro model for infections associated with medical implants, particularly indwelling catheters. Stressed cells initiating filamentation adhere quickly to nonpolar surfaces such as PDMS. In

397 practice, used squares that have been cleaned and resterilized in an autoclave (dry cycle) give
398 the most consistent biofilms for any particular strain. Biofilms also are commonly grown on cover
399 glasses, in cover glass bottom culture dishes, in standard bacteriological grade polystyrene
400 dishes, and on agar. Because *C. albicans* cells do not adhere well to glass, cover glasses should be
401 treated with a lectin that will bind cell wall polysaccharides. We apply 40 μL of 1 mg/mL ConA or
402 WGA in sterile water onto each coverslip surface. After drying, cover glasses are treated with 40
403 μL of 1% glutaraldehyde for 3 min to crosslink the protein into an insoluble film. They are then
404 washed with sterile distilled water to remove the fixative and any soluble lectin and air-dried. If
405 necessary, the treated cover glasses or dishes are resterilized under a germicidal UV lamp for 10
406 min.
407
408 Specimen thickness will affect the required incubation periods in the protocols. Fixative diffusion
409 into a 300 μm biofilm requires several minutes to equilibrate. This time period increases as the
410 square of the specimen thickens, and should be extended to an hour or more for very thick
411 biofilms or agar block specimens that may be 2–3 mm thick. The equilibration time period for
412 staining also depends on the specimen thickness as described for fixing and washout. However,
413 because the lectins diffuse more slowly than the low-MW fixatives, especially within an agar gel,
414 staining should be extended overnight. The same should be done for the washout of excess stain.
415
416 Stains of various types may be incorporated into the protocols. We use a cell wall stain for
417 structural imaging, most commonly Calcofluor White M2R (Fluor. Brightener #28) or a dye-tagged
418 lectin such as ConA-Alexafluor 594 or WGA-Alexafluor 594. Attention should be paid to the
419 valency of the protein. The ConA tetramer may cause crosslinking of highly flexible hyphae in the
420 apical region of a biofilm. This is less apparent with the WGA dimer. The canonical specificities of
421 these markers are Calcofluor for chitin, ConA for mannose residues, and WGA for N-acetyl-D-
422 glucosamine and sialic acid residues.
423
424 Because the solvent exchange protocol is graded from PBS or water though methanol into methyl
425 salicylate, specimen containers must be solvent-resistant. Methyl salicylate (MS) will quickly
426 soften polystyrene plasticware and slowly soften other plastics. The protocol steps up to the use
427 of the neat methanol can be carried out in plasticware, but at that point in the protocol we
428 generally switch over to standard 20 mL glass scintillation vials with solvent-resistant screw caps.
429 The vials are convenient for biofilms on silicone square substrata, because the squares can be
430 picked up and transferred using fine tweezers. Also, a vial can be drained and refilled with the
431 flat square resting on the inner curved surface so that the biofilm does not contact the glass. The
432 substratum should be biofilm-up when it is immersed in the upright vial. The vials are excellent
433 for long-term specimen storage.
434
435 In the clarification protocol, more graded solvent exchange steps minimize the risk of specimen
436 deformation due to solvent mixing effects. For speed and convenience in the basic protocol,
437 there are four steps: 1) step 3.3, PBS to 50:50 PBS:methanol; 2) steps 3.4 and 3.5, PBS:methanol
438 to neat methanol, 3) step 3.6, neat methanol to 50:50 methanol:MS; and 4) steps 3.7 and 3.8,
439 methanol:MS to neat MS. Methanol provides the transitional miscibility. However, because
440 water and MS are nearly immiscible, it is essential that all water be displaced by methanol prior

441 to the introduction of any MS. Likewise, because methanol is highly volatile, it is important to
442 displace all methanol by MS. Otherwise, the continued evaporation of residual methanol will
443 cause refractive index variations within the specimen. Within the four step sequence, repeating
444 the second and fourth steps by adding another change of neat solvent, or even a third change, is
445 advisable. For particularly fragile specimens, solvent changes could be formulated in smaller
446 percent steps.
447
448 With agar block specimens, steps 3.4 and 3.5 (neat methanol) may cause the appearance of salt
449 crystals within the agar due to the insolubility of residual PBS salts in the methanol. This can be
450 avoided by using distilled water (DW) in the first mixed solvent step in place of PBS to dilute salts
451 during the water:methanol exchange. The alternative solvent exchange sequence for fixed
452 biofilms then consists of the steps: 1) step 3.3, replace PBS with DW and use 50:50
453 DW:methanol; 2) step 3.4 use 50:50 DW:methanol instead of neat methanol (wash 2x with
454 methanol as in step 3.5); 3) step 3.6 replace methanol with 50:50 methanol:methyl salicylate;
455 and 4) step 3.7 use 50:50 methanol:MS (wash 2x with MS as in step 3.8).
456
457 Because methyl salicylate quickly softens polystyrene plasticware, we use an anodized aluminum
458 dish with a cover glass bottom to hold the clarified biofilm on the stage of an inverted
459 microscope. The cover glass is held in place using UV-curing optical cement (Norland Optical
460 Adhesive #61, see **Table of Materials**). Provided the MS is removed at the end of the day by
461 washing the dish with isopropanol followed by soapy water and rinsing, the cemented cover glass
462 will serve for many months.
463
464 Objective lens selection is critically important in large-scale imaging of clarified specimens
465 because of the importance of minimizing spherical aberration and the need for sufficient working
466 distance. We have experience with three objectives in these studies. In the inverted microscope
467 setup, we use a long working distance, a moderate numerical aperture (NA) objective oil
468 immersed below the cover glass with the biofilm immersed in methyl salicylate in the dish above
469 the cover glass. Most of our work has been done with a Zeiss Universal series achomatic
470 objective, type 461708, 40x 0.85NA Oel 160/1.5, used with a negative 160 mm focal length
471 adapter for nominal infinite-conjugate (IC) compatibility. This objective originally was designed
472 for oil immersed viewing through 1.5 mm microscope slides with 0.35 mm working distance[25].
473 When used with a standard cover glass (0.17 mm), the working distance is much greater: 1.5 +
474 0.35–0.17 = 1.68 mm = 1,680 µm. We also use a new Zeiss multi-immersion objective, type
475 420852, 25x 0.8NA LD LCI Plan-apochomat with a working distance exceeding 540 µm, with the
476 immersion correction set to the high side of 'oil'. This objective is highly corrected and produces
477 a superb image. On an upright microscope stand, we have used a new Nikon multi-immersion
478 objective, type MRD71120, 10x 0.5NA CFI Plan-apochomat with a working distance exceeding
479 5,000 µm (5 mm), also with the immersion correction set to the high side of 'oil' (n = 1.518).
480 Though this objective has a lower NA than the others, it has the advantage of being directly
481 immersible in methyl salicylate.
482
483 To optimize data acquisition in terms of speed and resolution, confocal microscope settings
484 ideally should meet both transverse and axial Nyquist sampling densities[18]. Using conventional

485   criteria, set the confocal pinhole diameter nominally to 1 Airy unit. In magnified coordinates,

486

487   d_P (µm) = 1.22 x magnification x (emission wavelength in µm) / NA

488

489   Transverse sampling (pixel spacing) should not exceed (1/2) x Abbe's resolution limit. In object-
490   space coordinates,

491

492   Δx, Δy = (emission wavelength in nm) / (4 NA)

493

494   Axial sampling (focus increment) should not exceed the inverse axial bandwidth,

495

496   Δz = (immersion index) x (emission wavelength in nm) / (NA^2)

497

498   The confocal optical system expands the bandwidth of the microscope and sharpens both the
499   transverse and axial resolution by at least 1/√2.

500

501   For the 40x 0.85 NA objective that we utilize most often, see **Table 1** for the results of these
502   formulas for a 600 nm emission wavelength (Alexa Fluor 594).

503

504   [Place **Table 1** here]

505

506   Using a spinning-disk confocal scanner with these settings and a 1,392 x 1,040 pixel scan field,
507   data from biofilm specimens can be acquired with reasonable speed and resolution. Typical
508   single-color 3D image stacks run 0.35–1.55 GB.

509

510   Clarification media in wide use span a significant refractive index range. By darkfield illumination
511   and visual inspection, we found that fixed *C. albicans* biofilms were most transparent above n =
512   1.5. This was refined by phase contrast microscopy to n = 1.530–1.535. For a number of practical
513   reasons, we use methyl salicylate (n = 1.537) as the final index matching solvent. Though solvent
514   exchange brings the risk of specimen deformation or other artifacts, cells in fixed, clarified
515   specimens have similar cell body dimensions, hypha diameter, and interseptal length dimensions
516   as live specimens.

517

518   Many variations in the solvent exchange process are possible (e.g., using a different transitional
519   solvent, or a different final solvent). Methanol was chosen for its high polarity and rapid diffusion,
520   but ethanol was shown to better preserve red fluorescent protein (RFP) quantum yield[26] as a
521   transitional solvent. Methyl salicylate was selected for its index, moderate polarity, low vapor
522   pressure, and compatibility with many stains, dyes, and fluorescent proteins. However, a final
523   solvent with slightly lower index, or a mixture of methyl salicylate and a lower index solvent such
524   as butanol, may work better.

525

526   Unexpectedly, the ability to see through a biofilm reveals not only its stratified internal features,
527   but also aids in viewing the origin of extended structures such as long, unentangled apical hyphae
528   and invasive basal hyphae on certain substrata. Opportunistic virulence in *C. albicans* depends

529 on its genetic versatility (i.e., switchover to hyphal growth, upregulation of cell substratum and
530 cell-cell adherence, generation of osmolytes for cell budding and elongation, and use of
531 alternative nutrients). Hyphal extension enables breakout of individual *C. albicans* cells from
532 phagocytic immune cells but also is essential for invasion. Biofilm adhesion and hyphal
533 entanglement appear to provide the surface anchoring needed for hyphae to efficiently invade a
534 substratum. When that substratum is host tissue, increased virulence may result.
535
536 Imaging intact biofilms enables a vast number of informative experiments utilizing reporter
537 strains for gene expression, model tissue substrata, and the inclusion of other organisms such as
538 bacteria found in natural biofilms. Even in the simplest case of purely structural imaging with a
539 cell wall stain, in situ phenotypes are revealed that then may be quantified and genetically
540 analyzed.
541

548 **DISCLOSURES:**
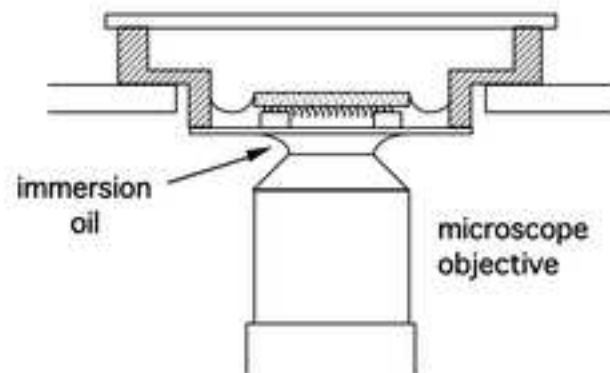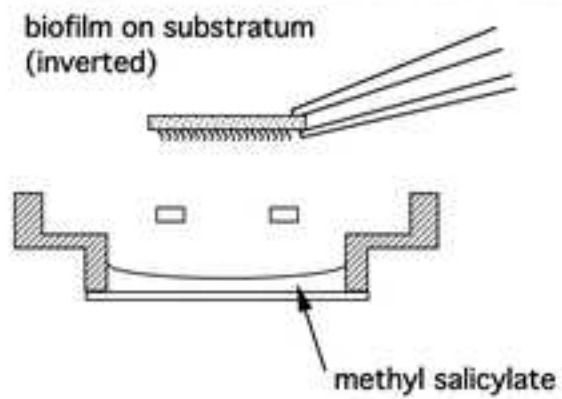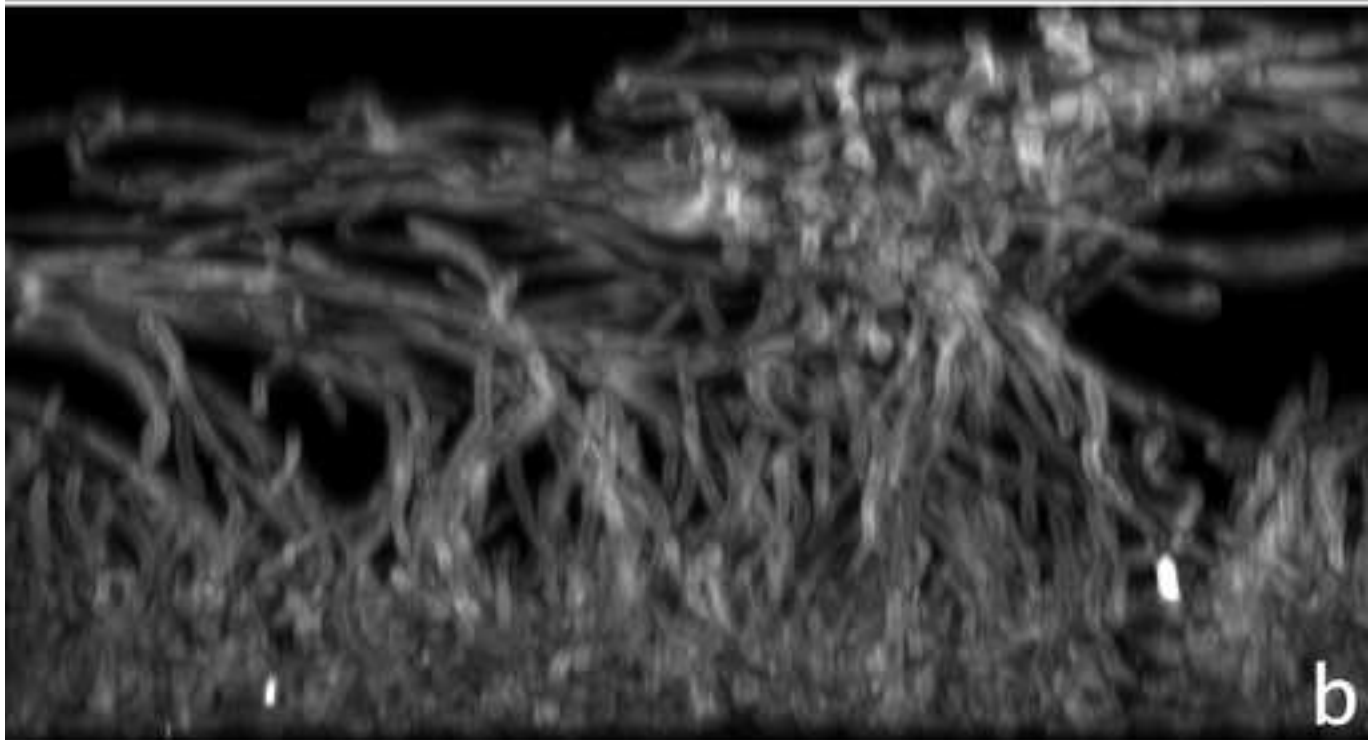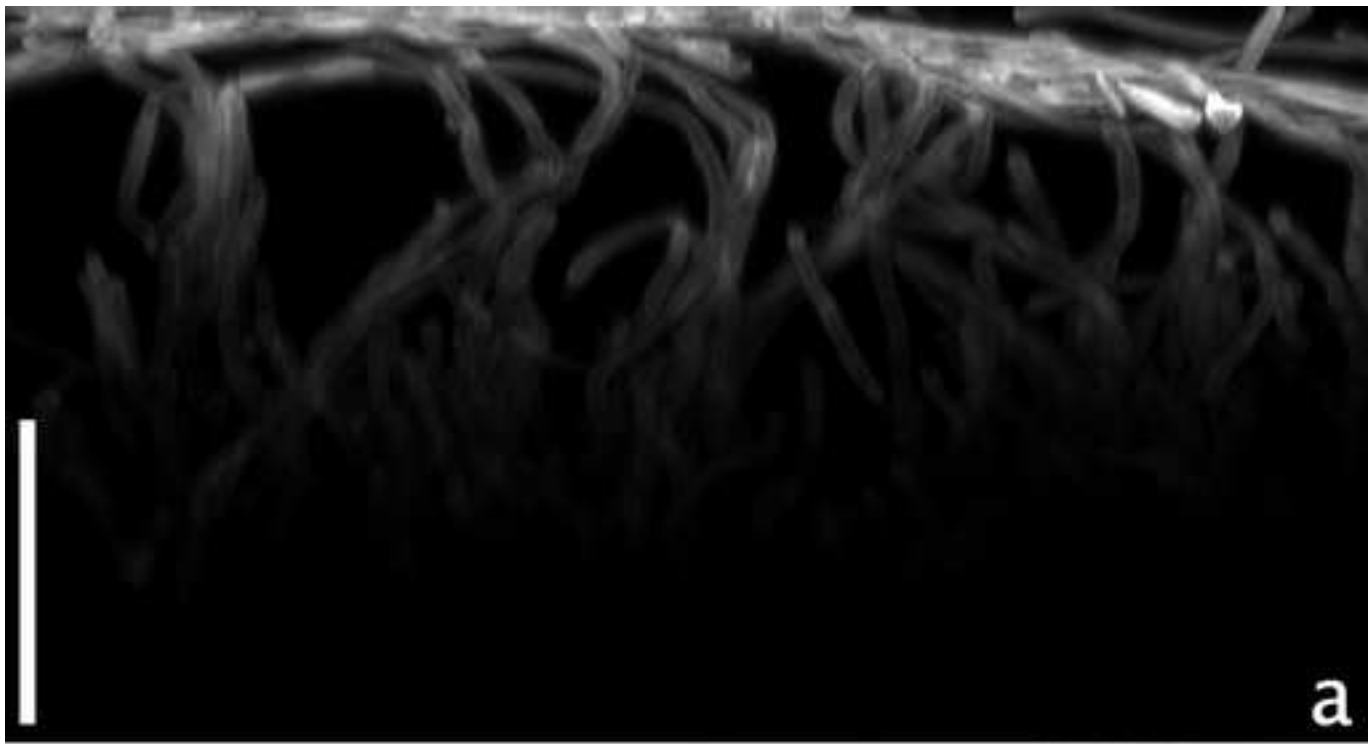549 The authors have no competing interests to disclose.
550

551 **REFERENCES:**
552 1. Desai, J. V. et al. Coordination of *Candida albicans* invasion and infection functions by
553 phosphoglycerol phosphatase Rh2. *Pathogens*. **4**, 573–589 (2015).
554 2. Miramón, P., Lorenz, M. C. A feast for *Candida*: Metabolic plasticity confers an edge for
555 virulence. *PLoS Pathogens*. **13**(2), e1006144 (2017).
556 3. Bonhomme, J. et al. Contribution of the glycolytic flux and hypoxia adaptation to efficient
557 biofilm formation by *Candida albicans*. *Molecular Microbiology*. **80**, 995–1013 (2011).
558 4. Ramírez-Zavala, B. et al. The Snf1-activating kinase Sak1 is a key regulator of metabolic
559 adaptation and in vivo fitness of *Candida albicans*. *Molecular Microbiology*. **104**, 989–1007
560 (2017).
561 5. Westman, J., Moran, G., Mogavero, S., Hube, B., Grinstein, S. *Candida albicans* hyphal
562 expansion causes phagosomal membrane damage and luminal alkalinization. *mBio*. **9**, e01226–
563 18 (2018).
564 6. Finkel, J. S., Mitchell, A. P. Genetic control of *Candida albicans* biofilm development. *Nature
565 Reviews Microbiology*. **9**, 109–118 (2011).
566 7. Finkel, J. S. et al. Portrait of *Candida albicans* adherence regulators. *PLoS Pathogens*. **8**,
567 e1002525 (2012).
568 8. de Groot, P. W., Bader, O., de Boer, A. D., Weig, M., Chauhan, N. Adhesins in human fungal
569 pathogens: glue with plenty of stick. *Eukaryotic Cell*. **12**, 470–81 (2013).
570 9. Lagree, K., Mitchell, A. P. Fungal Biofilms: Inside Out. Microbiology Spectrum 5 (2017).
571 10. Hawser, S. P., Douglas, L. J. Resistance of *Candida albicans* biofilms to antifungal agents in
572 vitro. *Antimicrobial Agents and Chemotherapy*. **39**, 2128–2131 (1995).

573 11. Chandra, J. et al. Biofilm formation by the fungal pathogen *Candida albicans*: development,
574 architecture, and drug resistance. *Journal of Bacteriology*. **183**, 5385–5394 (2001).
575 12. LaFleur, M. D., Kumamoto, C. A., Lewis, K. *Candida albicans* biofilms produce antifungal-
576 tolerant persister cells. *Antimicrobial Agents and Chemotherapy*. **50**, 3839–3846 (2006).
577 13. Lagree, K., Desai, J. V., Finkel, J. S., Lanni, F. Microscopy of fungal biofilms. *Current Opinion in*
578 *Microbiology*. **43**, 100–107 (2018).
579 14. Woolford, C. A. et al. Bypass of *Candida albicans* filamentation/biofilm regulators though
580 diminished expression of protein kinase Cak1. *PLoS Genetics*. **12**, e1006487 (2016).
581 15. Huang, M. Y., Woolford, C. A., May, G., McManus, C. J., Mitchell, A. P. Circuit diversification
582 in a biofilm regulatory network. *PLoS Pathogens*. **15**(5), e1007787 (2019).
583 16. Ganguly, S. et al. Zap1 control of cell-cell signaling in *Candida albicans* biofilms. *Eukaryotic*
584 *Cell*. **10**, 1448–1454 (2011).
585 17. Frisken, G. S., Lanni, F. Experimental test of an analytical model of aberration in an oil-
586 immersion objective lens used in three-dimensional light microscopy. *Journal of the Optical*
587 *Society of America*. **8**, 1601–1613 (1991). Reprinted in 9, 154–166 (1992).
588 18. Lanni, F., Keller, H. E. Microscope principles and optical systems. In *Imaging, A Laboratory*
589 *Manual*. Edited by Yuste RM. Cold Spring Harbor Laboratory Press (2011). pp. 1–55. Chapter 1.
590 19. Chung, K. et al. Structural and molecular interrogation of intact biological systems. *Nature*.
591 **497**, 332–337 (2013). (CLARITY)
592 20. Tomer, R., Ye, L., Hsueh, B., Deisseroth, K. Advanced CLARITY for rapid and high-resolution
593 imaging of intact tissues. *Nature Protocols*. **9**, 1682–1697 (2014).
594 21. Richardson, D. S., Lichtman, J. W. Clarifying tissue clearing. *Cell*. **162**, 246–257 (2015).
595 22. Chen, F., Tillberg, P. W., Boyden, E. S. Expansion microscopy. *Science*. **347**, 543–548 (2015).
596 23. Zhao, Y. et al. Nanoscale imaging of clinical specimens using pathology-optimized expansion
597 microscopy. *Nature Biotechnology*. **35**, 757–764 (2017).
598 24. Gao, R. et al. Cortical column and whole brain imaging with molecular contrast and nanoscale
599 resolution. *Science*. **363**, eaau8302 (2019).
600 25. "Optical Systems for the Microscope" publication 41–101-e (archive CZO-Mi 823, ed. 1967),
601 CARL ZEISS, 7082 Oberkochen, West Germany (1971). page 48.
602 26. Oldham, M., Sakhalkar, H., Oliver, T., Johnson, G. A., Dewhirst, M. Optical clearing of
603 unsectioned specimens for three-dimensional imaging via optical transmission and emission
604 tomography. *Journal of Biomedical Optics*. **13**(2), 021113 (2008).
605
606
607
608
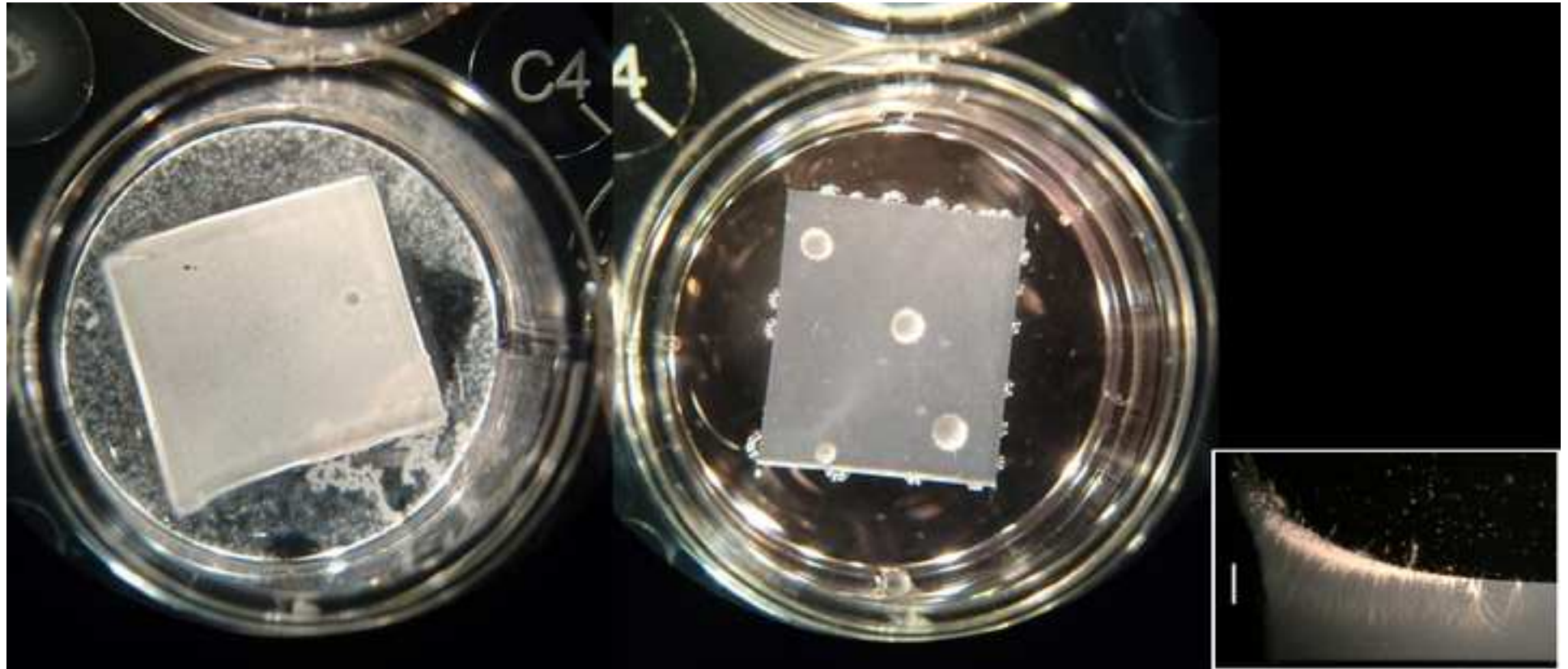
Figure 1

Figure 2

biofilm on substratum
(inverted)

methyl salicylate

immersion
oil

microscope
objective
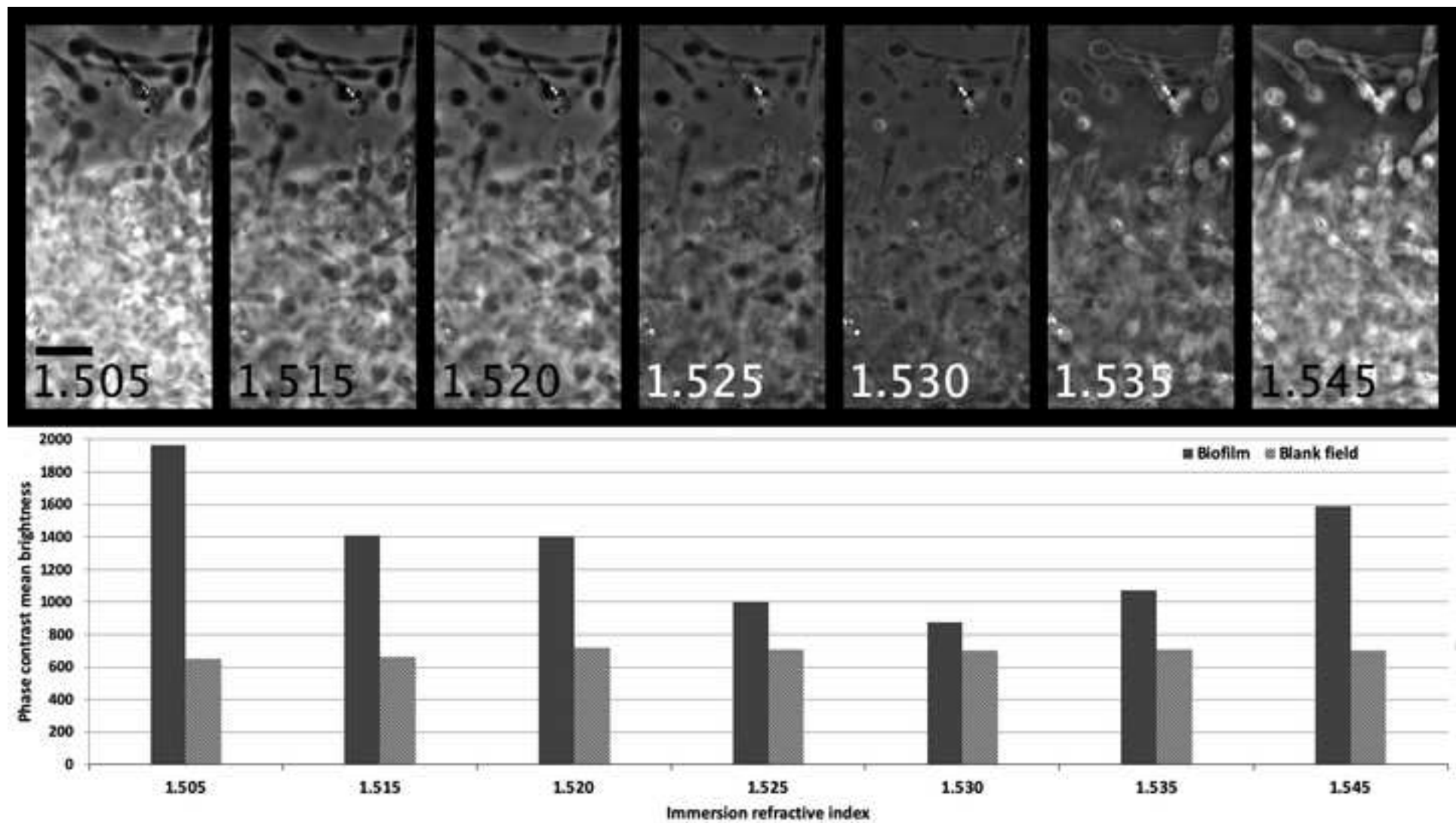
Figure 3

Figure 5

Table 1

	formula	x 1/√2	set (typical)	
d_P (μm)	34.5 μm	-	25 or 50 μm	
Δx, Δy	176 nm	125 nm	161 nm	-
Δz	1200 nm	848 nm	900 nm	
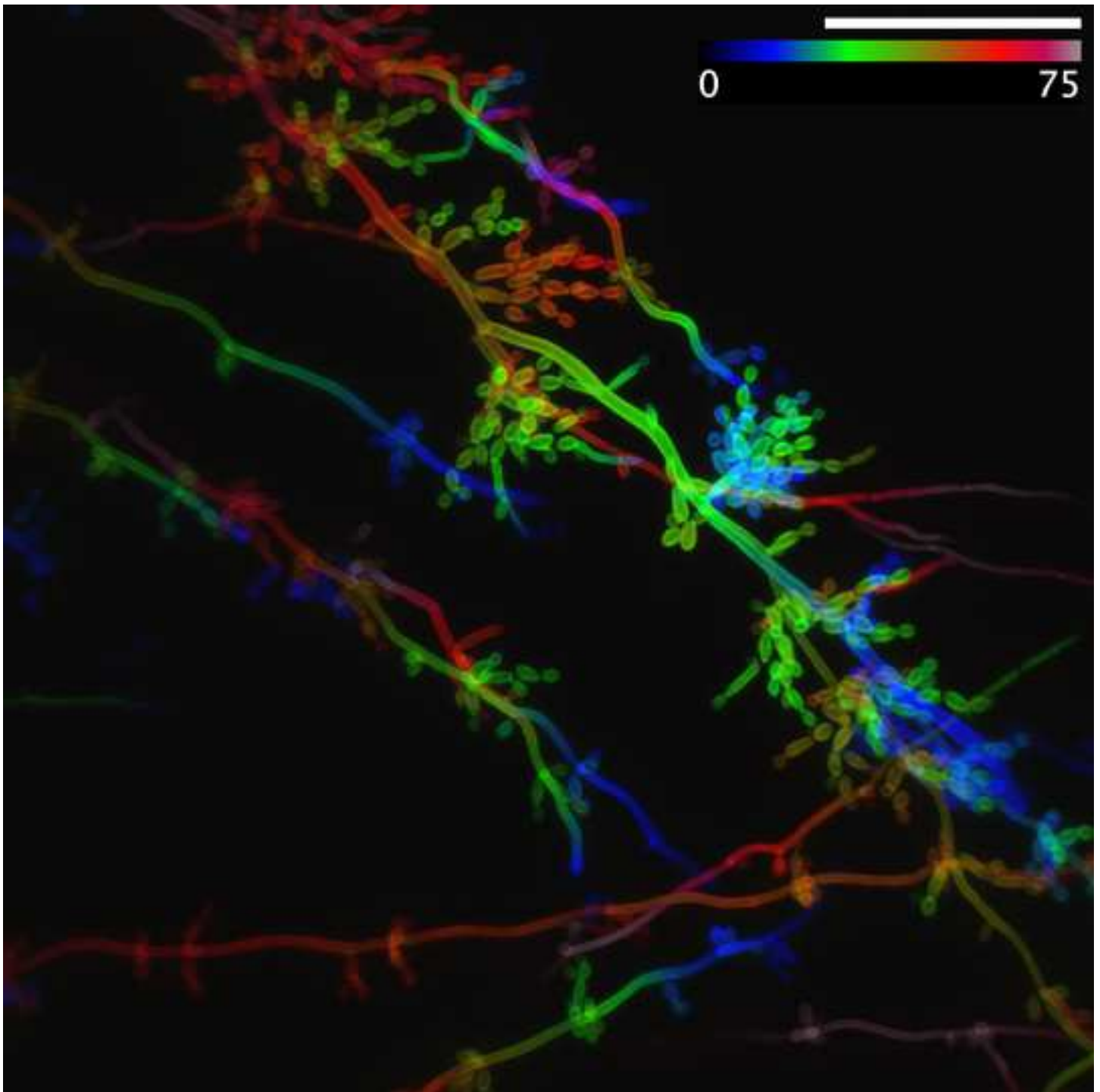
	formula	x 1/√2	set (typical)
d_P (μm)			25 or 50 μm

Name of Material/ Equipment	Company	contact	Catalog Number	Comments/Description
Biohazardous waste receptacle				
Biosafety cabinet with germicidal UV lamp				
Calcofluor White M2R (2.5 mg/mL in methanol)				
Concanavalin A - Alexafluor-594 or other conjugate				
Distilled water				DW
Distilled water, sterile				
Ethanol, absolute				EtOH
Fetal bovine serum (FBS), sterile				
Fixative waste bottle in secondary containment				
Formaldehyde 20% in water, ampules	Electron Microscopy Sciences			
Formaldehyde alternatives: paraformaldehyde powder, formalin 37%	Electron Microscopy Sciences			
Fume hood				
Glutaraldehyde 25% in water, ampules	Electron Microscopy Sciences			
Incubator - 30 deg C, with rotary mixer (60 rpm) for culture tubes				
Incubator - 37 deg C, with orbital mixer for culture plates				
Isopropanol 70%				iPrOH 70%
Longwave (365 nm) UV lamp, 5Watt	Cole-Parmer Scientific			for curing NOA-61 cement
Medical grade silicone sheet, 0.060" (1.52 mm) thick	Bentec Medical, Inc.	http://bentecmed.com/		Non-reinforced medical grade silicone sheeting
Methanol 99.9%				MeOH
Methyl salicylate 99%				MS
Millipore Swinnex 13mm white silicone ring gaskets	Millipore Corp.		SX0001301	
Norland UV-curing optical adhesive - type NOA-61	Edmund Optics, Inc.	https://www.edmundoptics.com	NOA-61	
Orbital mixer, benchtop				
Phosphate-buffered saline (PBS), sterile				
Refractive index standard liquids, n=1.500 to 1.640 (29 liquids, 0.005 increment)	Cargille Laboratories	https://cargille.com	Series E	Cedar Grove, NJ 07009, USA
RPMI-1640 base medium, HEPES buffered, sterile				
Scintillation vials, 20 mL - Wheaton, Urea cap PE cone cap liner	Fisher Scientific Co.		03-341-25H	for specimen processing and storage
Solvent waste bottle in secondary containment				
Spider medium with mannitol, sterile (1% Difco nutrient broth, 0.2% K2HPO4, 1% D-Mannitol)				
Wheat germ agglutinin - Alexafluor-594 or other conjugate				
Yeast-peptone-dextrose (YPD) agar plates, sterile (1% yeast extract, 2% Bacto peptone, 2% dextrose, 2% Bacto agar)				
YPD medium, liquid, sterile (1% yeast extract, 2% Bacto peptone, 2% dextrose)				

Carnegie Mellon

Department of Biological Sciences

Carnegie Mellon University
4400 5th Avenue
Pittsburgh, Pennsylvania 15213

14 October 2019

Phillip Steindel, Ph.D.
Review Editor
JoVE
1 Alewife Center
Cambridge MA 02140

Dear Dr. Steindel,

I have submitted the accompanying revised manuscript and figures, "Clarifying and Imaging *Candida albicans* Biofilms", for your review.

All text changes in the revision have been marked in red font.

The pages appended to this letter detail the changes that were made in response to your editorial instructions, and our responses to the many helpful comments of the four reviewers.

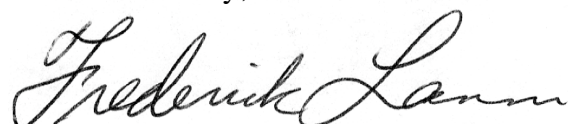We changed the title of the manuscript to the suggestion of Reviewer 4.

The biggest text change was removing the end notes from the four protocols, and rewriting this information into the Discussion.

The figure panels originally submitted have been combined into single figures (Figs. 1-5) as per your instructions. In my opinion, this is less satisfactory than separate panels. I will be happy to provide the individual panels, if your graphic artist agrees with me.

The content we suggest for videography runs from protocol step (2.3) through step (4.7), text lines 216-311. That is slightly over 2 pages in the revised manuscript.

Thank you for your patience, and your consideration of our research for your journal.

Sincerely,

Frederick Lanni, Ph.D.
Associate Professor

e-mail: lanni@cmu.edu   phone: 412-268-3460   http://www.cmu.edu/bio/faculty/primary/lanni.html

Changes in v9 document from v8:

version identifier: REVISION / v9e / 14oct2019
line numbering turned on.
Text changes are marked in red font throughout.

<u>Changes in response to Editorial Comments:</u>

General:
Changed to single line spacing in all paragraphs.
Changed to Calibri 12-point font throughout.
Corrected all instances of "um" to "μm".
<mark>Content for videography</mark>:   Protocol steps (2.3) through (4.7).
                        Text lines 216-311, mainly manuscript pages 5-6.

Introduction:
wording changes: line 80
                      line 152

Protocols:
Removed all end notes (Notes) from protocols 1-4. The information in the Notes now appears as new text in the Discussion - paragraphs 2-10.

line 220: changed wording: extend time period when processing thicker specimens.

Representative results:
lines 332-336: Figure 1 legend has been revised.
lines 339-348: Figure 2 legend has been revised. Sentence on schematic diagram has been added. Other figure legends have minor revisions.

Discussion:
line 407: added text

lines 410-539: <u>Inserted text from 4 sets of end notes removed from the individual protocols.</u> These notes were revised to constitute Discussion paragraphs 2-10. New text is in red font. References to these paragraphs were inserted into the protocols.

lines 564-565: changed wording: biofilm adhesion and hyphal entanglement appear to provide the surface anchoring needed for hyphae to efficiently invade a substratum.

lines 569-571: added text.

Figures:
Removed embedded figures from text.
Figure 1: Dropped Figure 1(a) and combined the remaining two panels at the same scale. Updated the legend.
Figure 2: Added schematic panel to Figure 2 in response to Reviewer #2, and updated legend.
Figure 3: Combined 3a and 3b, and updated legend.

Figure 4: Combined 4a, 4b, and 4c, and updated the legend.
Figure 5: Added axial scale color bar, updated legend.

Acknowledgements: updated

References:
lines 584-690: Put citations in standard format.
Citations 19-27 were re-ordered and renumbered.

Table of Materials: updated

Changes in response to Reviewer comments:

We thank the four Reviewers for their comments, suggestions, and corrections.

Reviewer #1:
corrected all instances of 'hyphus' to 'hypha'.

Reviewer #2:
The biggest disadvantage of our approach is that it isn't applicable to living specimens. Because that is apparent, we don't see the need to state it. We do state that the method is intended for fixed specimens in the Short Abstract, in the Abstract, and twice in the Introduction! We also didn't really include a paragraph on advantages - such as not having to cut serial sections, and register images afterward. Again, that is apparent, therefore no need to state explicitly. In the Introduction (lines 140-162), we specifically address some intrinsic difficulties of our approach.

The reviewer correctly points out the need for specialty objectives. We have updated our discussion of long working distance immersion microscope objectives in the text (see lines 490-539). In the original manuscript, we described two Zeiss objectives used in our work - one an obsolete model (40x 0.85NA), and one a modern multi-immersion lens (25x 0.8NA) that is readily obtainable. To address this point further, we tested a modern Nikon long working distance multi-immersion objective (10x 0.5NA) which can be directly immersed in methyl salicylate and other clarifying solvents. Information on this objective is included in the revised text. (lines 503-507)

Reviewer #2 line items:
1. We wrote the first paragraph to summarize relevant common knowledge. Citations start immediately in 2nd paragraph.

2. micron symbol corrected throughout.

3. lines 152 and 555: added reference to use of butanol (n = 1.399) to adjust refractive index.

4. Yes, we agree. Glutaraldehyde definitely increases broadband autofluorescence (and also strongly attenuates dTomato fluorescence). That has not been a problem in most of our work, but particularly affects quantitative imaging with GFP and RFP tags. We feel that this is widely known, and therefore didn't address the problem in the original text. We have added a note on glutaraldehyde in the protocol (2.2) - lines 213-214.

5. We've always used formalin or formaldehyde at 4% for mammalian cell work, where its action is more or less instantaneous, as seen by live-cell microscopy. To limit osmotic effects and autofluorescence, we keep the fixative concentration as low as possible. We have used formalin in the 4-10% concentration range with no noticeable difference in results.

6. The suggested diagram has been added as a panel in Figure 2.

7. line 301: defined "INA".

8. lines 317-318: Changes made as suggested. References to Fig. 2 and Fig. 3 have been made explicit.

9. line 327: changed terminology to 'lateral budding yeast' as suggested.

10. line 332: added title/caption to Figure 1.

11. Figure 2: references to the figure panels have been corrected.

12. Figure 2 legend: Yes, direct water immersion = dipping objective, as opposed to indirect water immersion through a coverglass.

13. Figures 2 and 4c graphic errors corrected.

14. Figure 4 legend: DAY185 is the wild-type strain used as a control in Woolford, *et al* (cited as #14). Its origin can be traced back from that paper to a 2000 paper by Davis, *et al*. Since that earlier paper is not directly related to the current manuscript, we believe that citing Woolford *et al* is sufficient here.

15. Figure 5 legend: The color scale depth range was added to the legend as text.

16. lines 544-545: The term 'visual immersion refractometry' has been replaced with 'By darkfield illumination and visual inspection'.

Reviewer #3:
The reviewer is correct - The images in Figure 2 do not appear as sharp as in the high-resolution figures (Figs. 4 and 5). In the 63x water-immersion image, that is due to the refraction of light by the cells in the biofilm. The MS immersion image was enlarged from 40x to match the magnification of the water-immersion image. That involved some interpolation which 'softened' its appearance. However, these images show clearly the main benefit of clarification.

Reviewer #4:
Changed title of article as suggested: Clarifying and Imaging *Candida albicans* Biofilms

---